

## Systematics of low-lying dipole strengths in odd and even Dy and Gd isotopes

J. Margraf, T. Eckert, M. Rittner, I. Bauske, O. Beck, U. Kneissl, H. Maser, H. H. Pitz, and A. Schiller  
*Institut für Strahlenphysik, Universität Stuttgart, Allmandring 3, D-70569 Stuttgart, Germany*

P. von Brentano, R. Fischer, R.-D. Herzberg, N. Pietralla, and A. Zilges  
*Institut für Kernphysik, Universität zu Köln, Zùlpicher Str. 77, D-50937 Köln, Germany*

H. Friedrichs\*

*Institut für Kernphysik, Justus-Liebig-Universität Giessen, Leihgesterner Weg 217, D-35392 Giessen, Germany*

(Received 31 May 1995)

Photon scattering experiments on the odd, deformed nuclei  $^{161,163}\text{Dy}$  and  $^{157}\text{Gd}$  provided detailed information on the excitation energies and transition probabilities of low-lying dipole excitations. In the case of the even-even nuclei  $^{162,164}\text{Dy}$  in addition spins and parities of the excited states could be determined model independently by measuring the angular distributions and the linear polarization of the scattered photons using a Compton polarimeter. The results are compared with the systematics obtained for the neighboring even-even isotopes  $^{160}\text{Dy}$  and  $^{156,158,160}\text{Gd}$  in previous photon scattering experiments. Whereas in the odd Dy isotopes a concentration of dipole strength is observed, which fits nicely into the systematics of the orbital  $M1$  mode, the dipole strength in  $^{157}\text{Gd}$  is completely fragmented into about 90 transitions.

PACS number(s): 25.20.Dc, 23.20.Js, 23.20.Lv, 27.70.+q

### I. INTRODUCTION

Low-lying dipole excitations in heavy nuclei are of great interest in modern nuclear structure physics. Nuclear resonance fluorescence (NRF), photon scattering off bound states, represents a highly selective and sensitive tool to investigate these low-lying dipole excitations [1]. The discovery of a new class of enhanced *magnetic* dipole excitations in heavy deformed nuclei in high resolution electron scattering experiments by Richter and co-workers [2] opened a new field in nuclear spectroscopy and initiated a large number of both experimental and theoretical work [3–10]. This low-lying, predominantly orbital mode, often referred to as the *scissors mode*, today is known as a rather general phenomenon in deformed even-even nuclei of the rare earth and actinide mass region. These isovector  $M1$  excitations, which originally have been predicted in the framework of the two-rotor model [11] and discussed in the proton-neutron version of the interacting boson model (IBM-2), nowadays can be explained microscopically by quasiparticle random phase approximation (QRPA) calculations, performed by several groups (for references see, e.g., [3–5,7,12,13]).

The systematics and fragmentation of the  $M1$  strength in the rare earth *even-even* nuclei is well established by systematic electron, photon, and proton scattering experiments (see, e.g., [6,7]). NRF data are available for different Nd, Gd, Dy, Er, Yb, and W isotopes obtained by the Stuttgart-Giessen-Cologne collaboration (see [6] and references therein) and Sm nuclei investigated by the Darmstadt group [14,15]. The total  $M1$  strength  $B(M1)\uparrow$  in the energy range 2.6 – 4 MeV reaches a saturation value around midshell of  $\approx 3\mu_N^2$ . The qualitative behavior of saturation is the same as observed for the systematics of  $B(E2)$  values in this mass region [16] and

has also been observed in the other region of strongly deformed nuclei, the actinides [17]. The rise of the summed  $M1$  strength from spherical to well-deformed nuclear shapes has been studied in detail in the Sm [14,15] and Nd isotopic chains [18,19]. It turned out that the summed  $M1$  strength scales with the square of the nuclear deformation parameter  $\delta$  (“ $\delta^2$  law”) [14]. This behavior can be explained by different theoretical approaches (for references see [15]) and is one of the most exciting findings in the last years.

Recently, LoIudice and Richter [20] derived a new, simple sum rule for the  $M1$  strength of the scissors mode:

$$B(M1)\uparrow \approx 0.0042 \frac{4NZ}{A^2} \omega_{\text{Sc}} A^{5/3} (g_p - g_n)^2 \delta^2 [\mu_N^2] \quad (1)$$

with  $\omega_{\text{Sc}}$  the energy of the *scissors mode* ( $\approx 3$  MeV),  $\delta$  the nuclear deformation parameter, and the  $g$  factors  $g_n=0$  and  $g_p=2Z/A$ . This formula contains no free parameters and predicts the absolute strength for the scissors mode. There is an excellent agreement with the experimental data, ranging from the hardly deformed Nd and Sm nuclei to the well-deformed Gd and Dy isotopes (see [6,7]). Only the results for the W isotopes [21] and for Hf nuclei fall below the sum rule predictions and hint to a reduced  $M1$  strength in these nuclei at the transition from axially symmetric rotors to more  $\gamma$ -soft rotors [22]. The overall exhaustion of the sum rule by the experimentally observed strength points to the fact that in the photon scattering experiments nearly all orbital  $M1$  excitations in these nuclei have been observed.

In odd, deformed nuclei a fragmentation of the orbital  $M1$  strength is expected due to different couplings of the unpaired nucleon to each of the  $M1$  excitations in the even-even core and due to the mixing with single-particle levels. A first photon scattering experiment on the odd-proton nucleus  $^{165}\text{Ho}$  by the Darmstadt group [23] showed no strong excitations in the region around 3 MeV. Theoretically, the orbital

\*Present address: Deutsche Bank, 65760 Eschborn.

$M1$  strength should be separated more clearly from the single particle excitations in nuclei with an odd neutron number. Therefore, at the Stuttgart facility the odd-neutron isotope  $^{163}\text{Dy}$  was investigated [24], which has the additional advantage that in both neighbouring even-even nuclei the strength is concentrated in two or three very strong excitations [25–27]. The observed concentration of dipole strength in excitation energy around 3 MeV fits into the systematics of the scissors mode in the neighboring even-even Dy isotopes. Furthermore, recent calculations in the framework of the interacting boson fermion model (IBFM) support the interpretation of these excitations as a first observation of the scissors mode in an *odd* nucleus [24].

The aim of the present investigations was twofold. First of all, the existence of the scissors mode in *odd* nuclei and its fragmentation should be established by further measurements on  $^{161}\text{Dy}$  and  $^{157}\text{Gd}$ . Both odd isotopes are neighbors of strongly deformed even-even nuclei within the well-investigated Dy and Gd isotopic chains [2,25–31]. In the even-even isotopes  $^{162,164}\text{Dy}$  NRF experiments of improved sensitivity including the measurement of the linear polarization of the scattered photons should enable model independent parity assignments and provide information on the fragmentation of the scissors mode in these isotopes. In addition, the parity determinations allow to identify and to study in more detail low-lying *electric* dipole excitations in the energy range 1–4 MeV. Enhanced  $E1$  transitions are expected and observed in deformed nuclei [32–40,26]. These excitations can be interpreted in terms of different collective excitation modes [32] or two-phonon excitations [33,41]. In Sec. II the experimental method of the nuclear resonance fluorescence technique is explained in some detail. Section III shows the experimental setup at the Stuttgart Dynamitron. In Secs. IV and V the obtained results are presented and discussed.

## II. NUCLEAR RESONANCE FLUORESCENCE TECHNIQUE

Nuclear resonance fluorescence (NRF) represents the resonant absorption of real photons exciting a nuclear level and its decay by reemission of a photon. Due to the small momentum of real photons only dipole and with much smaller probability  $E2$  transitions are induced. This spin selectivity enables dipole excitations to be investigated in energy regions, where the level density is already very high. The use of a continuous photon source, such as bremsstrahlung, allows the strength distribution of dipole excitations to be measured simultaneously in detail in the energy interval covered by the photon source [1].

The cross section  $\sigma$  for the absorption and subsequent reemission of a photon from the ground state with spin and parity  $J_0^\pi$  to some excited state ( $J^\pi$ ) and back to the ground state or a low-lying state ( $J_f^\pi$ ) is measured. The resonance shape of the cross section is of Doppler-broadened Breit-Wigner type. Since a continuous photon source (bremsstrahlung) is used the energy integrated cross section  $I_s$  is determined in the NRF experiments:

$$I_s = \frac{2J+1}{2J_0+1} \left( \frac{\hbar c}{E_\gamma} \right)^2 \frac{\Gamma_0 \Gamma_f}{\Gamma} \frac{W(\Theta)}{4\pi}, \quad (2)$$

$J$  and  $J_0$  are the spins of the excited and ground state, respectively, and  $W$  the angular distribution.  $\Gamma_0$ ,  $\Gamma_f$ , and  $\Gamma$  are the decay widths to the ground state, to the final level, and the total decay width, respectively. In the case of elastic scattering ( $\Gamma_0 = \Gamma_f$ ) the scattering cross section is proportional to  $\Gamma_0^2/\Gamma$ . If the decay to other states can be observed or is known, then the ground state width  $\Gamma_0$  can be determined.  $\Gamma_0$  is proportional to the reduced transition probabilities  $B(\Pi L, E_\gamma) \uparrow$  ( $\Pi = E$  or  $M$ ):

$$\Gamma_0 = 8\pi \sum_{\Pi L=1}^{\infty} \frac{(L+1)(E_\gamma/\hbar c)^{2L+1}}{L[(2L+1)!!]^2} \frac{2J_0+1}{2J+1} \times B(\Pi L, E_\gamma) \uparrow. \quad (3)$$

The angular correlation function  $W(\Theta)$  of the scattered photons  $\gamma_2$  with respect to the incoming photon  $\gamma_1$  (beam) (measured by polarization insensitive devices), restricting ourselves to the reasonable cases  $L_n \leq 2$ , can be written as [42]

$$W(\Theta) = \sum_{\nu=0,2,4} A_\nu(1) A_\nu(2) P_\nu(\cos\Theta). \quad (4)$$

The expansion coefficients are given by

$$\begin{aligned} A_\nu(1) &= \left( \frac{1}{1+\delta_1^2} \right) \{ F_\nu(L_1 L_1 J_i J) + 2\delta_1 F_\nu(L_1 L_1' J_i J) \\ &\quad + \delta_1^2 F_\nu(L_1' L_1' J_i J) \}, \\ A_\nu(2) &= \left( \frac{1}{1+\delta_2^2} \right) \{ F_\nu(L_2 L_2 J_f J) + 2\delta_2 F_\nu(L_2 L_2' J_f J) \\ &\quad + \delta_2^2 F_\nu(L_2' L_2' J_f J) \}. \end{aligned} \quad (5)$$

Here  $J_i = J_0$ ,  $J$ , and  $J_f$  are the spins of the initial (in NRF ground states), intermediate, and final states, respectively.  $L_n$ ,  $L'_n$  (with  $L'_n = L_n + 1$ , and  $n = 1, 2$ ) refer to the multipolarities of the transitions involved. The mixing ratios  $\delta_n$  are defined as usual:

$$\delta_n = \frac{\langle \psi_f | L_{n+1} | \psi_i \rangle}{\langle \psi_f | L_n | \psi_i \rangle}. \quad (6)$$

The  $F$  coefficients can be found in various compilations (e.g. [43,44]).

In the case of even-even nuclei the spins of the excited states can be determined easily from the measured angular distributions, since only pure dipole or quadrupole cascades with spin sequences 0-1-0 or 0-2-0 occur. It is sufficient to measure the scattered radiation at least at two different angles. The most favorable configuration is  $\Theta = 90^\circ$  and  $127^\circ$ . The intensity ratio  $W(90^\circ)/W(127^\circ)$  amounts to 0.734 and 2.28 for dipole and quadrupole transitions, respectively. These values are slightly reduced for realistic geometries and finite solid angles used in the experiments [29].

Unfortunately, in the case of odd- $A$  nuclei the angular distributions are, due to the half-integer spins involved, nearly isotropic. Therefore, it is difficult to extract conclusive

information on the spins of the excited levels. This can be achieved in the present setup only in a few favorable cases (e.g.,  $J_0 = 1/2$ ) [24].

The photon-excited states can decay to the ground state or to low-lying excited states (with spins  $J_0$  and  $J_f$ , respectively). The ratio of the corresponding reduced transition probabilities defines the branching ratio  $R_{\text{expt}}$ .

$$R_{\text{expt}} = \frac{\Gamma_{J_f} E_{\gamma J_0}^3}{\Gamma_{J_0} E_{\gamma J_f}^3} = \frac{B(J \rightarrow J_f)}{B(J \rightarrow J_0)}. \quad (7)$$

In the rotational limit for deformed nuclei the branching ratio  $R_{\text{theo}}$  is given by

$$R_{\text{theo}} = \left| \frac{\sqrt{2J_f+1} \langle J_f, K_f, L, K - K_f | J, K \rangle}{\sqrt{2J_0+1} \langle J_0, K_0, L, K - K_0 | J, K \rangle} \right|^2 \quad (8)$$

and allows the  $K$  quantum number  $K$  of the excited state to be measured assuming the validity of these so-called Alaga rules [46].

In the case of even-even nuclei the photon-excited states have spin 1 and can decay to the  $0^+$  ground state or the first excited  $2^+$  state. For the decay of  $J=1$  states into the ground state band of deformed nuclei, one expects within the validity of the Alaga rules  $B(1 \rightarrow 2)/B(1 \rightarrow 0) = 2$  or  $0.5$  for  $K=0$  or  $K=1$  states, respectively. For odd- $A$  nuclei the branching ratio can provide some valuable information on the spin of the photoexcited state.

In the case of a polarization sensitive detector for the scattered photon  $\gamma_2$ , like a Compton polarimeter, the angular distribution function [Eq. (4)] depends additionally on the angle  $\gamma$  between the electric field vector  $\vec{E}$  and the reaction plane ( $\gamma_1 - \gamma_2$ ). The linear polarization correlation function can be written as [42]

$$W(\Theta, \gamma) = W(\Theta) + (\pm)_{L'_2} \sum_{\nu=2,4} A_\nu(1) A'_\nu(2) \times P_\nu^{(2)}(\cos\Theta) \cos(2\gamma) \quad (9)$$

with

$$A'_\nu(2) = \left( \frac{1}{1 + \delta_2^2} \right) \{ -\kappa_\nu(L_2 L_2') F_\nu(L_2 L_2' J_f J) + 2\delta_2 \kappa_\nu(L_2 L_2') F_\nu(L_2 L_2' J_f J) + \delta_2^2 \kappa_\nu(L_2' L_2') F_\nu(L_2' L_2' J_f J) \}. \quad (10)$$

The unnormalized associated Legendre polynomials  $P_\nu^{(2)}$  and the coefficients  $\kappa_\nu(L_n, L_n')$  are given in [42]. The factors  $(\pm)_{L'_2}$  are  $+1$  and  $-1$  for electric and magnetic transitions, respectively. The degree of linear polarization  $P(\Theta)$  is defined by the relative difference of the scattering cross sections resulting in radiation with the electric field vector  $\vec{E}$  parallel and perpendicular to the reaction plane ( $\gamma_1 - \gamma_2$ ) and follows from Eq. (9):

$$P(\Theta) = \frac{(\pm)_{L'_2} \sum_{\nu=2,4} A_\nu(1) A'_\nu(2) P_\nu^{(2)}(\cos\Theta)}{\sum_{\nu=0,2,4} A_\nu(1) A_\nu(2) P_\nu(\cos\Theta)}. \quad (11)$$

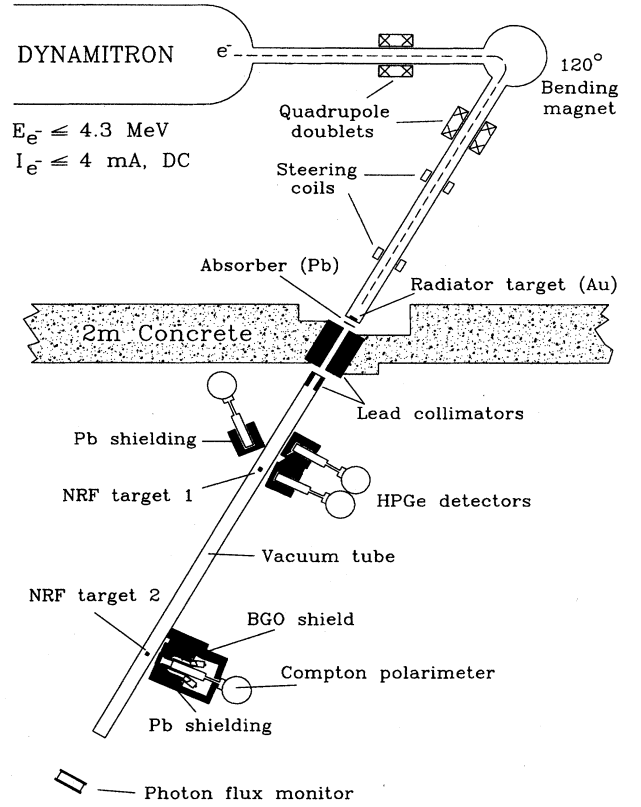


FIG. 1. The bremsstrahlung facility at the Stuttgart Dynamitron accelerator [29,45]. The excellent quality of the well-collimated bremsstrahlung beam allows one to run two NRF experiments simultaneously. At the first setup the angular correlation and cross section measurements take place, while at the second setup the polarization measurements are performed (see text).

The experimentally observed asymmetry  $\varepsilon(\Theta)$  as measured using a polarimeter with a polarization sensitivity  $Q$  amounts to

$$\varepsilon(\Theta) = P(\Theta) Q(E_\gamma). \quad (12)$$

The polarization sensitivity  $Q(E_\gamma)$  of a Compton polarimeter arrangement (including its apparatus asymmetries) can be determined experimentally using  $\gamma-\gamma$  cascades with known spins and mixing ratios or using photons of known linear polarization from appropriate  $(p, p' \gamma)$  reactions [47].

In the most important and favorable cases of pure dipole or quadrupole transitions (elastic scattering off even-even nuclei; spin sequences 0-1-0 or 0-2-0) the maximal polarization of  $|P|=1$  is observed for a scattering angle  $\Theta = 90^\circ$ . The angular distributions for electric and magnetic dipole transitions are identical, however, the sign of the polarization changes. This enables model independent parity assignments for levels in even-even nuclei. For odd nuclei, as mentioned above, the angular distributions are nearly isotropic. Therefore, following Eq. (11), the degree of polarization  $P(\Theta)$  is nearly zero and parity assignments are *not* possible.

TABLE I. Target compositions and specifications.

Isotope	Composition	Enrichment (%)	Total masses (mg)		Major impurities
			Isotope	$^{27}\text{Al}$	
$^{164}\text{Dy}$	$\text{Dy}_2\text{O}_3$	96.0	4805	1510	$^{163}\text{Dy}$ (2.7%); $^{162}\text{Dy}$ (0.8%)
	Dy metal	95.6	1052		$^{163}\text{Dy}$ (1.9%); $^{162}\text{Dy}$ (2.2%)
$^{163}\text{Dy}$	$\text{Dy}_2\text{O}_3$	92.8	2777	517	$^{164}\text{Dy}$ (4.5%); $^{162}\text{Dy}$ (2.1%)
$^{161}\text{Dy}$	$\text{Dy}_2\text{O}_3$	92.1	1834	765	$^{162}\text{Dy}$ (5.5%); $^{163}\text{Dy}$ (1.2%)
$^{157}\text{Gd}$	$\text{Gd}_2\text{O}_3$	92.3	1850	510	$^{158}\text{Gd}$ (5.4%); $^{156}\text{Gd}$ (1.9%)

### III. EXPERIMENTAL SETUP

The NRF measurements reported on have been performed at the bremsstrahlung facility of the Stuttgart Dynamitron accelerator [29,45]. The setup is shown schematically in Fig. 1. The high current dc electron beam with a maximum energy of 4.3 MeV is bent by  $120^\circ$  and focused on the bremsstrahlung radiator target consisting of a water cooled gold plate thick enough to completely stop the electrons. The resulting bremsstrahlung beam is formed by a lead collimator with a hole of 10 mm diameter and 98 cm length. The radiation production is well separated from the experimental setups by 2 m of concrete, resulting in a low level of background radiation. The photon beam is guided in a vacuum tube to the NRF setups. The excellent beam quality and the very high flux of typically  $10^6$  photons per keV and second for 3 MeV photons enable to run NRF experiments at two different setups simultaneously.

The first NRF site consists of three carefully shielded Ge(HP) detectors placed at scattering angles of  $90^\circ$ ,  $127^\circ$ , and  $150^\circ$  with respect to the incident beam. At the second site the sectored Ge(HP) Compton polarimeter is installed at slightly backward angles of  $97^\circ$  with respect to the photon beam for background reasons. This detector measures the polarization of the resonantly scattered photons utilizing the Compton effect. The outer electrode of this true coaxial germanium crystal is carved into four electrically insulated surfaces, dividing the crystal into four detectors. This enables, by requiring coincidence conditions between the four segments, the measurement of the direction of the Compton scattering in the detector and thus the polarization of the photons. The device is described in detail in [47]. Its polarization sensitivity determined in  $(p, p' \gamma)$  reactions amounts to  $\approx 20\%$  at 0.5 MeV and remains  $\approx 9.5\%$  at 4.4 MeV. The overall detection sensitivity of the polarimeter could recently be increased considerably by improving its response function using a BGO anti-Compton shield [48].

For both setups the NRF targets consist of pills of isotopically enriched material sandwiched between aluminum disks of the same diameter. Typically 1–2 g of enriched isotopes are needed for setup 1 and 5 g for the polarization measurements. The target compositions and specifications are summarized in Table I. The nucleus  $^{27}\text{Al}$  has three well-known excitations [49] between 2 and 4 MeV, which serve for several on-line calibration purposes in these experiments. Due to the half-integer spins, the photons from the 2982 keV excitation are emitted nearly isotropically and are nearly unpolarized. They serve as an on-line calibration for the angular distribution and the polarization. In addition, the well-known decay widths and decay branching ratios of the levels

at 2212, 2982, and 3957 keV are used for the photon flux calibration. The results are in very good agreement with Monte Carlo calculations of the bremsstrahlung shape [50] and experimental determinations. Furthermore, the measurement of the NRF cross section relative to the excitations in  $^{27}\text{Al}$  eliminates all effects due to changes in beam energy and intensity. The accuracy of the measured cross sections is mainly limited by the error of the aluminum standard. Therefore, we recently performed a NRF self-absorption experiment on these levels [51], to determine absolutely the corresponding total widths  $\Gamma$  (or lifetimes). The obtained results are in excellent agreement with the literature values [49]. In

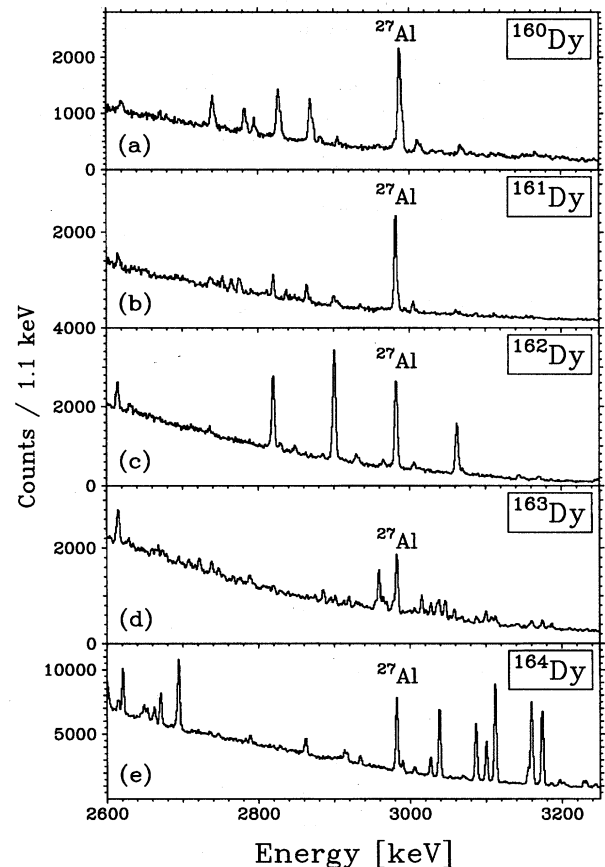


FIG. 2. Photon scattering spectra off  $^{160,161,162,163,164}\text{Dy}$  in the energy range of the scissors mode, measured at a scattering angle of  $90^\circ$ , see text.

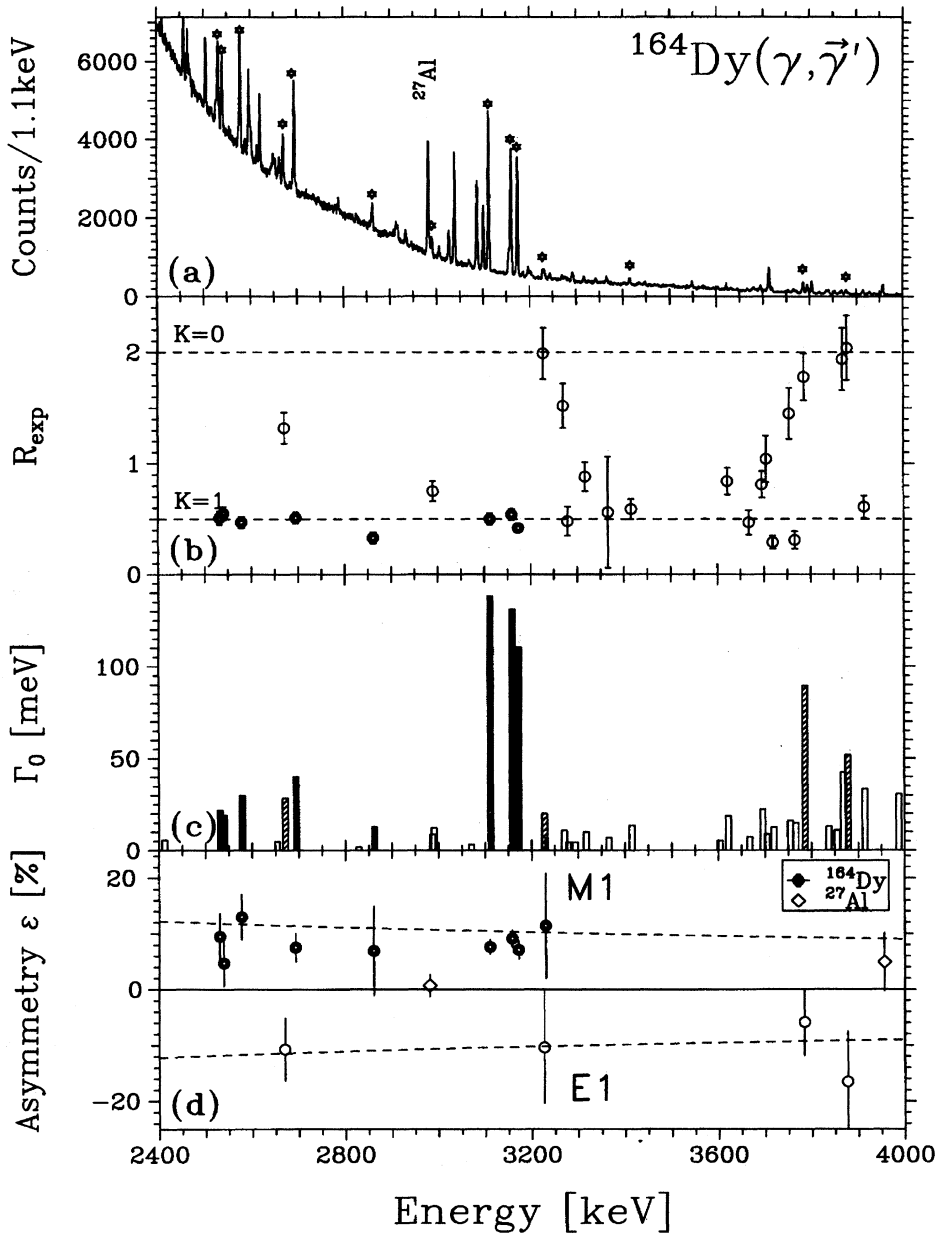


FIG. 3. Results for the  $(\gamma, \gamma')$  experiment on  $^{164}\text{Dy}$ . (a) Spectrum of photons detected at a scattering angle of  $90^\circ$ . Peaks marked by Al belong to the photon flux standard, peaks marked by an asterisk belong to strong ground state transitions in  $^{164}\text{Dy}$ , see text. (b) Experimentally observed decay branching ratios  $R_{\text{expt}}$  for the decays to the first excited state and the ground state. The lines marked with  $K=0$  and  $K=1$  give the values expected from the Alaga rules [46]. Full symbols correspond to  $M1$  transitions with determined parities. (c) Ground state decay widths  $\Gamma_0$  extracted from the present experiment. Full bars belong to  $M1$  transitions, shaded bars to  $E1$  transitions. Open bars indicate that no parity could be extracted from the present polarization measurements. (d) Azimuthal asymmetry  $\epsilon$  of the scattered photons measured with the Compton polarimeter. The dashed lines give the expectation values for completely linearly polarized photons. Positive asymmetries correspond to  $M1$  transitions, negative asymmetries to  $E1$ .

particular, we succeeded in cutting the error for the width of the most important level at 2982 keV to 2.4%.

#### IV. EXPERIMENTAL RESULTS

##### A. Results for the Dy isotopes $^{161,162,163,164}\text{Dy}$

Figure 2 shows a general view of the measured spectra of photons scattered off various Dy isotopes (at a scattering angle of  $90^\circ$ ). It is evident that the spectra for the even isotopes are dominated by a few strong transitions, whereas numerous weaker transitions were observed for the odd nuclei (the strong line in all spectra marked by  $^{27}\text{Al}$  belongs to a well known transition in  $^{27}\text{Al}$  used for the photon flux calibration). Already this figure demonstrates the needed increased experimental sensitivity when investigating odd isotopes in NRF experiments.

Figure 3 shows the experimental data for  $^{164}\text{Dy}(\gamma, \gamma')$  as a typical example for the information obtained from photon scattering experiments on even-even nuclei. In the upper part the spectrum of photons is depicted scattered under  $90^\circ$  with respect to the incoming photon beam. Once again the strong line marked by  $^{27}\text{Al}$  belongs to a transition in the photon flux standard  $^{27}\text{Al}$ . Peaks marked by an asterisk correspond to ground state transitions in  $^{164}\text{Dy}$ . Each ground state transition is accompanied by a satellite peak 73 keV lower in energy, which stems from the decay of the excited state to the first  $J^\pi=2^+$  level of the ground state rotational band. The intensity ratio of these two decay branches contains the information on the  $K$  quantum number. This can be seen in the second part of Fig. 3, where the experimentally observed branching ratios  $R_{\text{expt}}$  are plotted. The dashed horizontal lines marked with  $K=0$  and  $K=1$  give the values expected

TABLE II. Results for the reaction  $^{162}\text{Dy}(\gamma, \gamma')$ . The measured excitation energies  $E_x$ , the integrated scattering cross sections  $I_s$ , decay branching ratios  $R_{\text{expt}}$ , and azimuthal asymmetries  $\epsilon$  are summarized. From these quantities the ground state transition widths  $\Gamma_0$ , the spins and parities  $J^\pi$ , the  $K$  quantum numbers and reduced transition probabilities  $B(M1)\uparrow$  and  $B(E1)\uparrow$  were deduced and given in the table.

$E_x$ (keV)	$I_s$ (eV b)	$\Gamma_0$ (meV)	$R_{\text{expt}}$	$\epsilon$ (%)	$K$	Spin $J^\pi$	$B(M1)\uparrow$ ( $\mu_N^2$ )	$B(E1)\uparrow$ ( $10^{-3} e^2 \text{ fm}^2$ )
2395	$36.3 \pm 1.9$	$27.3 \pm 1.6$	$0.57 \pm 0.03$	$16.3 \pm 7.6$	1	$1^+$	$0.52 \pm 0.03$	-
2520	$22.9 \pm 1.4$	$27.7 \pm 2.0$	$1.31 \pm 0.08$	$-14.6 \pm 8.3$	(0,1)	$1^-$	-	$5.0 \pm 0.4$
2537	$5.1 \pm 0.9$	$3.6 \pm 0.7$	$0.29 \pm 0.13$	-	1	$1^?$	$0.06 \pm 0.01$	$0.63 \pm 0.01$
2569	$10.9 \pm 1.0$	$8.7 \pm 0.9$	$0.43 \pm 0.08$	$16.5 \pm 13.6$	1	$1^+$	$0.13 \pm 0.01$	-
2815	$4.7 \pm 1.2$	$6.1 \pm 1.8$	$0.98 \pm 0.31$	-	0	$1^?$	$0.07 \pm 0.01$	$0.78 \pm 0.01$
2900	$144 \pm 9$	$153 \pm 9$	$0.50 \pm 0.02$	$10.2 \pm 3.3$	1	$1^+$	$1.63 \pm 0.10$	-
2909	$3.7 \pm 0.9$	$7.6 \pm 2.3$	$1.95 \pm 0.53$	-	0	$1^?$	$0.08 \pm 0.02$	$0.88 \pm 0.02$
2929	$12.6 \pm 1.1$	$14.6 \pm 1.4$	$0.61 \pm 0.08$	$-8.1 \pm 13.7$	1	$1^-$	-	$1.7 \pm 0.2$
2965	$8.8 \pm 1.0$	$9.6 \pm 1.2$	$0.46 \pm 0.10$	$20.2 \pm 19.1$	1	$1^+$	$0.10 \pm 0.01$	-
3061	$90.6 \pm 6.1$	$95.0 \pm 8.2$	$0.31 \pm 0.08$	$8.9 \pm 4.2$	1	$1^+$	$0.86 \pm 0.08$	-

from the Alaga rules [46]. The full symbols correspond to  $M1$  transitions for which the positive parities could be determined by the present polarization measurements. It is evident that the three very strong excitations around 3.1 MeV have branching ratios  $R_{\text{expt}} \approx 0.5$ . This determines the  $K$  quantum number to  $K = 1$  for the excited levels. This is expected for the mixed symmetry  $J^\pi = 1^+$  states of the scissors mode. In the third part of Fig. 3 the strength distribution (ground state transition widths  $\Gamma_0$ ) is plotted. Full bars correspond to  $M1$  transition, shaded bars to  $E1$  transitions. Open bars belong to dipole transitions for which no parities could be determined. The parity assignments come from the present measurements of the linear polarization of the scattered photons using a Compton polarimeter. The measured azimuthal asymmetries  $\epsilon$  are shown in the lowest part of Fig. 3. The dashed lines correspond to the expected asymmetries for completely polarized photons and are given by the polarization sensitivity  $Q(E_\gamma)$  of the polarimeter [47]. Positive asymmetries correspond to  $M1$  excitations and negative asymmetries are expected for  $E1$  excitations. In the figure full circles belong to  $M1$  transitions, open circles to  $E1$  transitions. The open rhombs show the data points for the nearly unpolarized transitions in  $^{27}\text{Al}$ . These data are in agreement with an asymmetry  $\epsilon \approx 0$ , which proves the good apparatus symmetry of the polarimeter device. There are clearly two groups of strong  $M1$  excitations around 2.5 and 3.1 MeV, respectively. The upper group is attributed to the scissors mode. In the Tables II and III the numerical results of the NRF experiments including linear polarization are summarized. The excitation energies  $E_x$  of the observed dipole transitions are given together with the corresponding integrated scattering cross sections  $I_s$ , the ground state transition widths  $\Gamma_0$ , the decay branching ratios  $R_{\text{expt}}$  and the azimuthal asymmetries  $\epsilon$  measured by the Compton polarimeter device (for the stronger transitions). The assigned  $K$  quantum numbers, spins and parities  $J^\pi$ , and the extracted reduced transition probabilities  $B(M1)\uparrow$  and  $B(E1)\uparrow$  are quoted in the last four columns of both tables. In the case of the odd isotopes  $^{163,161}\text{Dy}$  due to the half-integer spins of the levels involved and the resulting nearly isotropic angular distributions it was not possible to determine the spins and parities of the excited levels in the present photon scattering

experiments. Therefore, the products  $g\Gamma_0$  of the ground state transition widths  $\Gamma_0$  and the spin factors  $g = (2J+1)/(2J_0+1)$  are given together with the excitation energies  $E_x$ , the observed integrated scattering cross sections  $I_s$  and the decay branching ratios  $R_{\text{expt}}$ . Furthermore, the final states are quoted to which decays from the photoexcited states could be detected (the ground states of  $^{163}\text{Dy}$  and  $^{161}\text{Dy}$  have spins of  $5/2^-$  and  $5/2^+$ , respectively). The given reduced transition probabilities  $B(M1)\uparrow$  were calculated under the assumption of  $M1$  excitations and do not depend on the spin of the excited state.

### B. Results for $^{157}\text{Gd}$

The results for  $^{157}\text{Gd}$ , the third odd-neutron nucleus, which was investigated in the present  $(\gamma, \gamma')$  experiments, differ dramatically from those observed for the odd Dy isotopes. Already the raw data show no concentration of dipole strength but an extreme fragmentation. This can be seen in Fig. 4 where the  $(\gamma, \gamma')$  spectra for the reactions  $^{161}\text{Dy}(\gamma, \gamma')$  and  $^{157}\text{Gd}(\gamma, \gamma')$  are compared. Peaks belonging to transitions in the photon flux standard ( $^{27}\text{Al}$ ), target impurities ( $^{162}\text{Dy}$ ), or background ( $^{208}\text{Pb}$ ) are marked by the corresponding symbols. Whereas in the upper spectrum for  $^{161}\text{Dy}$  a clear concentration of dipole excitations around 2.8 MeV is visible, for  $^{157}\text{Gd}$  no strong excitations could be observed. A detailed analysis [52] of all data, taken in two separate experimental runs, each measuring under 3 scattering angles simultaneously, revealed data for in total 90 excitations. The numerical results are summarized in Table IV. The given quantities are the same as in Tables V and VI. The quoted reduced transition probabilities are calculated assuming negative parities ( $M1$  excitations).

## V. DISCUSSION

### A. $M1$ strength distributions in the Dy isotopes $^{160,161,162,163,164}\text{Dy}$

The even-even Dy isotopes  $^{160,162,164}\text{Dy}$  have been investigated already in 1988 in high resolution photon scattering experiments at the Stuttgart facility [25]. A concentration of dipole strength near 3 MeV, in the energy range of the scis-

TABLE III. Results for the reaction  $^{164}\text{Dy}(\gamma, \vec{\gamma}')$ . The quoted quantities are explained in the caption of Table II.

$E_x$ (keV)	$I_s$ (eV b)	$\Gamma_0$ (meV)	$R_{\text{expt}}$	$\epsilon$ (%)	$K$	Spin $J^\pi$	$B(M1)$ ( $\mu_N^2$ )	$B(E1)$ ( $10^{-3} e^2 \text{fm}^2$ )
1675	44.69±4.23	28.3± 3.5	1.83±0.24	-23.2± 8.3	0	1 <sup>-</sup>	-	17.24±2.13
1841	5.90±1.05	3.6± 0.8	1.24±0.31	-	(0,1)	1 <sup>- a</sup>	-	1.67±0.37
2052	3.60±0.70	3.0± 0.7	1.43±0.35	-	0	1 <sup>- a</sup>	-	1.00±0.24
2330	23.16±1.93	29.4± 3.3	1.87±0.22	-10.5± 4.9	0	1 <sup>-</sup>	-	6.67±0.74
2412	3.23±0.51	5.7± 1.2	2.73±0.51	-	0	1 <sup>- a</sup>	-	1.16±0.24
2531	27.52±2.12	22.5± 1.9	0.51±0.06	9.5± 4.1	1	1 <sup>+</sup>	0.360±0.031	-
2540	23.59±1.83	19.8± 1.7	0.55±0.06	4.7± 4.1	1	1 <sup>+</sup>	0.314±0.027	-
2578	36.94±2.80	30.4± 2.5	0.47±0.05	13.0± 4.1	1	1 <sup>+</sup>	0.460±0.038	-
2653	7.76±0.72	4.7± 0.4	-	-	-	-	0.066±0.006	0.73±0.07
2671	20.75±1.58	28.4± 2.7	1.32±0.14	-10.7± 5.6	(0,1)	1 <sup>-</sup>	-	4.27±0.41
2694	43.93±3.23	40.7± 3.3	0.51±0.05	7.5± 2.5	1	1 <sup>+</sup>	0.539±0.044	-
2828	2.52±0.44	1.8± 0.3	-	-	-	-	0.020±0.003	0.22±0.04
2862	14.32±1.12	13.3± 1.1	0.33±0.05	6.9± 8.0	1	1 <sup>+</sup>	0.147±0.012	-
2986	3.39±0.53	8.5± 1.7	2.43±0.43	-	0	1 <sup>- a</sup>	-	0.92±0.18
2990	9.26±0.73	12.2± 1.1	0.75±0.09	-	1	1 <sup>+ b</sup>	0.118±0.011	-
3027	17.07±1.16	13.6± 0.9	-	-	-	-	0.127±0.009	1.40±0.10
3070	3.79±0.44	3.1± 0.4	-	-	-	-	0.028±0.003	0.31±0.04
3112	112.48±7.14	138.6± 9.9	0.50±0.05	7.6± 1.3	1	1 <sup>+</sup>	1.192±0.085	-
3159	101.03±6.48	131.7± 9.4	0.54±0.05	9.1± 1.5	1	1 <sup>+</sup>	1.083±0.077	-
3173	91.78±5.90	111.3± 7.7	0.42±0.04	7.1± 1.6	1	1 <sup>+</sup>	0.903±0.062	-
3185	3.35±0.42	3.0± 0.4	-	-	-	-	0.024±0.003	0.26±0.03
3228	7.70±0.70	19.9± 2.3	1.99±0.23	-10.4± 9.6	0	1 <sup>-</sup>	-	1.69±0.20
3231	7.22±0.67	6.6± 0.6	-	11.4± 9.4	-	-	0.050±0.005	0.56±0.05
3270	4.83±0.50	10.9± 1.4	1.52±0.20	-	(0)	1 <sup>- a</sup>	-	0.89±0.12
3279	3.15±0.47	4.3± 0.7	0.48±0.13	-	1	1 <sup>+ b</sup>	0.031±0.005	-
3293	4.68±2.02	4.4± 1.9	-	-	-	-	0.032±0.014	0.35±0.15
3316	5.65±0.60	9.9± 1.2	0.88±0.13	14.5±16.5	(1)	1 <sup>(+)</sup>	0.070±0.009	-
3365	4.60±0.96	6.9± 2.5	0.56±0.50	-	1	1 <sup>+ b</sup>	0.047±0.017	-
3414	8.61±0.80	13.5± 1.5	0.59±0.09	-	1	1 <sup>+ b</sup>	0.088±0.009	-
3603	4.59±0.57	5.2± 0.6	-	-16.7±16.7	-	-	0.029±0.004	0.32±0.04
3621	3.85±0.62	12.6± 2.6	2.00±0.38	-	0 <sup>c</sup>	1	0.069±0.014	0.76±0.15
3667	4.35±0.57	7.3± 1.1	0.47±0.11	-	1	1	0.038±0.006	0.43±0.06
3695	10.61±1.13	18.1± 2.1	0.47±0.08	-	1 <sup>c</sup>	-	0.093± 0.011	1.03±0.12
3704	3.74±0.55	8.8± 1.6	1.04±0.21	-	(0,1)	1 <sup>- a</sup>	-	0.50±0.09
3718	8.15±0.82	12.5± 1.4	0.29±0.06	17.1±11.5	1	1 <sup>+</sup>	0.063± 0.007	-
3754	5.55±0.67	16.1± 2.4	1.45±0.23	-	(0)	1 <sup>- a</sup>	-	0.87±0.13
3765	9.32±0.93	14.9± 1.7	0.31±0.08	-	1	1 <sup>+ b</sup>	0.072± 0.008	-
3785	26.83±2.31	89.4±10.2	1.78±0.21	-5.9± 5.9	0	1 <sup>-</sup>	-	4.72±0.54
3836	10.10±1.09	12.9± 1.4	-	-	-	-	0.059± 0.006	0.65±0.07
3853	8.44±0.95	10.9± 1.2	-	-	-	-	0.049± 0.006	0.54±0.06
3868	11.55±1.25	42.5± 6.1	1.94±0.28	-	0	1 <sup>- a</sup>	-	2.11±0.30
3877	13.56±1.41	51.9± 7.2	2.04±0.29	-16.5± 9.0	0	1 <sup>-</sup>	-	2.55±0.35
3914	4.89±0.98	18.7± 4.7	1.98±0.46	-	0 <sup>c</sup>	1 <sup>- a</sup>	-	0.89±0.22
3987	6.34±1.02	23.9± 5.0	1.83±0.38	-	0 <sup>c</sup>	1 <sup>- a</sup>	-	1.08±0.23

<sup>a</sup>Tentative parity assignment based on  $K=0$ .<sup>b</sup>Tentative parity assignment based on  $K=1$ .<sup>c</sup>Chain of transitions enfolded under the assumption of certain  $K$  numbers.

sors mode, could be detected in these experiments. Positive parities were proposed from the  $K=1$  assignments and comparison with  $(e, e')$  data for  $^{164}\text{Dy}$  [27,53] at low and high transfers of momentum. The present NRF experiments on  $^{162,164}\text{Dy}$ , including linear polarization measurements, confirmed these parity assignments and, furthermore, the ex-

tracted strengths are in perfect agreement with the previous NRF data [25]. Due to the improved sensitivity and the much longer measuring times in the polarization measurements weaker transitions could be detected and the overall uncertainties could be reduced. This confirmation of the previous NRF results [25] gives further confidence into these data, in

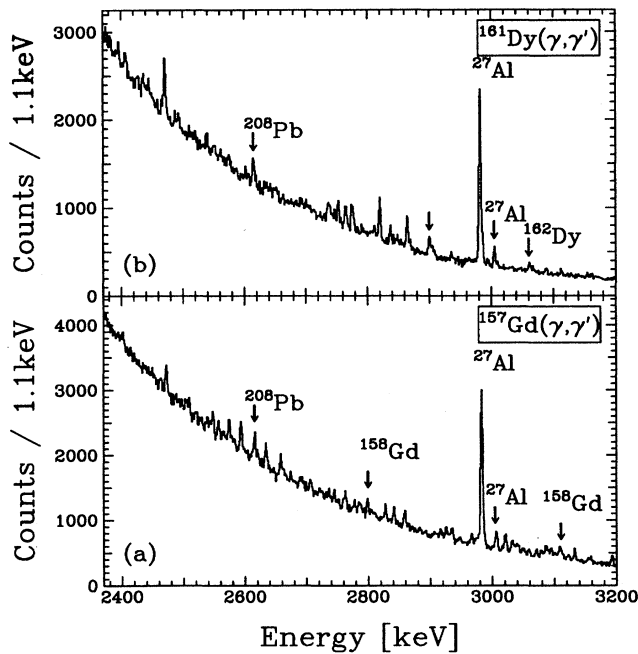


FIG. 4. Comparison of the photon scattering spectra off the odd neutron nuclei  $^{161}\text{Dy}$  and  $^{157}\text{Gd}$ . Calibration lines ( $^{27}\text{Al}$ ), lines from room background ( $^{208}\text{Pb}$ ) and from target impurities ( $^{162}\text{Dy}$ ,  $^{158}\text{Gd}$ ) are marked.

particular in view of the lower  $B(M1)$  values reported from a recent  $(n,n'\gamma)$  experiment [54]. This is even more noteworthy, since the  $(n,n'\gamma)$  data for  $^{162}\text{Dy}$  [54] are in a good agreement with the NRF results from [25] and the present work.

The summed  $B(M1)\uparrow$  strengths for  $^{162,164}\text{Dy}$  in the energy range of the scissors mode are in a good agreement with the systematics of observed  $M1$  strengths in the even-even rare earth nuclei [6] (for  $^{164}\text{Dy}$  the measured total  $M1$  strength has been reduced by the amount of  $M1$  spin contributions as measured in intermediate energy proton scattering by Frekers *et al.* [55]). The group of  $M1$  excitations in  $^{164}\text{Dy}$  around 2.5 MeV is not included in the systematics of the scissors mode, because a  $^{165}\text{Ho}(t,\alpha)$  experiment [56] reported a nearly pure two-quasiparticle  $M1$  excitation in this energy region. It should be emphasized that the measured summed  $B(M1)$  strengths [6] are in a nearly complete agreement with the values given by the sum rule recently derived by LoIudice and Richter [20] [Eq. (1)].

After these systematic investigations of the even-even Dy isotopes the question of the existence of the scissors mode in odd nuclei and its expected fragmentation were studied in the present NRF experiments on  $^{163,161}\text{Dy}$  performed at the Stuttgart facility [24,57]. These problems have been studied theoretically by Van Isacker and Frank [58,59] in the framework of the interacting boson fermion model (IBFM) and in the particle-core coupling model by Raduta *et al.* [60]. The theoretical works predict a fragmentation of the orbital  $M1$  strength due to different couplings of the unpaired nucleon to each of the  $M1$  excitations in the even-even core and due to the mixing with single particle levels.

Figure 5 shows the strength distributions for all five investigated Dy isotopes. For even-even nuclei the ground state transition widths  $\Gamma_0$  for  $\Delta k=1$  transitions are plotted. For transitions marked by crosses the parities are known from the present polarization measurements to be positive. For the odd isotopes the products  $g\Gamma_0$  are depicted since the spins of the excited states could not be determined, as discussed above. One states that for both odd isotopes  $^{163}\text{Dy}$  and  $^{161}\text{Dy}$  the energetic position as well as the magnitude of summed strengths ( $\Sigma\Gamma_0$  and  $\Sigma g\Gamma_0$ , respectively, given in the right corners of the figures) fit quite well into the systematics in the neighboring even-even nuclei. However, it should be noted that if one compares the summed  $B(M1)\uparrow$  strengths, the total strengths observed in the odd isotopes seem to be reduced by a factor of roughly 3 as compared to the even-even nuclei.

For  $^{163}\text{Dy}$  the data can be compared with recent theoretical IBFM calculations [24] as given in Table VII. Inspection of the second column shows that for different spins of the excited states different decay branching ratios are expected. If the experimental data are classified according to this scheme, the respective number of states and their summed strengths can be calculated. There is obviously a good agreement between experiment and theory, so that a first observation of the scissors mode in a deformed odd- $A$  nucleus can be stated. This interpretation is supported by the new measurements on  $^{161}\text{Dy}$  [57]. These studies complete the experiments on the Dy isotopic chain. The strength in  $^{161}\text{Dy}$  is somewhat more fragmented than in  $^{163}\text{Dy}$  and the centroid is shifted to lower energies. However, both, strengths and energies, fit well into the systematics. This is true not only for the excitations near 3 MeV but also for the group around 2.5 MeV.

#### B. $M1$ strength distributions in the Gd isotopes $^{156,157,158,160}\text{Gd}$

As already shown in Fig. 4 where the photon scattering spectra for  $^{161}\text{Dy}$  and  $^{157}\text{Gd}$  were compared, the dipole strength distribution is dramatically different in  $^{157}\text{Gd}$ . This is shown in more detail in Fig. 6, where the dipole strength distribution in  $^{157}\text{Gd}$  is compared with the data for the well-investigated neighboring, even-even Gd isotopes. As in Fig. 5 the ground state transition widths  $\Gamma_0$  and  $g\Gamma_0$  are plotted. For marked transitions in even Gd isotopes the positive parities are known from electron scattering experiments (open symbols [28,31]) and NRF polarization measurements (full symbols [30]). The dipole strength in  $^{157}\text{Gd}$  is distributed over more than 90 transitions in the whole energy range 2–4 MeV where the present NRF experiments have a good sensitivity. Furthermore, the total sum  $\Sigma g\Gamma_0$  is higher than in the neighboring even-even Gd isotopes, in contrast to the observations in the odd Dy isotopes. Since in  $^{157}\text{Gd}$  more than 100 transitions (including inelastic transitions) have been observed in the energy interval 2–4 MeV it cannot be ruled out completely that by chance two ground state transitions are separated by the energy of an excited level. This can lead to a misinterpretation of one of these ground state transitions (the lower energetic one) as a branching to the respective excited level. But this would have no influence on the general conclusions drawn here.

TABLE IV. Results for the reaction  $^{157}\text{Gd}(\gamma, \gamma')$ . Results for the excitation energies  $E_x$ , the integrated cross sections  $I_s$ , and the reduced transition probabilities  $B(M1)\uparrow$  are given. All states decay to the ground state ( $J^\pi=3/2^-$ ). If a decay branching to another low-lying state (besides the ground state) was observed, the branching ratio  $R_{\text{expt}}$  and the spin and parity  $J_f^\pi$  of this final state is given in columns 4 and 5, respectively.

$E_x$ (keV)	$I_s$ (eV b)	$g_J\Gamma_0$ (meV)	$R_{\text{expt}}$	Final state $J_f^\pi$	$B(M1)\uparrow^a$ ( $\mu_N^2$ )
1956	2.55±0.39	2.54±0.39	-	-	0.029±0.004
1976	1.73±0.36	1.76±0.37	-	-	0.020±0.004
2073	3.58±0.41	4.01±0.45	-	-	0.039±0.004
2131	3.28±0.37	3.87±0.44	-	-	0.035±0.004
2180	1.73±0.32	2.14±0.39	-	-	0.018±0.003
2200	4.23±0.38	5.33±0.48	-	-	0.043±0.004
2250	1.91±0.50	2.51±0.67	-	-	0.019±0.005
2253	1.45±0.35	1.92±0.46	-	-	0.015±0.003
2290	2.14±0.33	2.92±0.45	-	-	0.021±0.003
2306	2.01±0.29	2.78±0.40	-	-	0.020±0.003
2335	1.82±0.30	2.58±0.43	-	-	0.018±0.003
2346	1.59±0.36	2.27±0.51	-	-	0.015±0.003
2397	1.57±0.28	2.35±0.42	-	-	0.015±0.003
2402	1.67±0.28	2.51±0.41	-	-	0.016±0.003
2446	1.24±0.28	1.93±0.44	-	-	0.011±0.003
2488	2.10±0.30	3.38±0.48	-	-	0.019±0.003
2504	2.32±0.28	3.78±0.46	-	-	0.021±0.003
2509	1.74±0.31	2.84±0.50	-	-	0.016±0.003
2519	1.02±0.29	1.68±0.47	-	-	0.009±0.003
2527	1.62±0.36	2.70±0.60	-	-	0.014±0.003
2537	1.80±0.30	3.02±0.50	-	-	0.016±0.003
2542	1.76±0.35	2.96±0.59	-	-	0.016±0.003
2547	3.11±0.32	5.25±0.55	-	-	0.027±0.003
2556	2.13±0.29	3.62±0.49	-	-	0.019±0.003
2564	1.58±0.31	2.71±0.54	-	-	0.014±0.003
2581	1.23±0.33	2.14±0.57	-	-	0.011±0.003
2592	3.37±0.30	5.89±0.53	-	-	0.029±0.003
2594	2.99±0.28	5.24±0.50	-	-	0.026±0.002
2633	4.87±0.38	8.87±0.69	-	-	0.042±0.003
2657	3.81±0.33	7.01±0.61	-	-	0.032±0.003
2674	1.78±0.25	6.76±1.04	1.11 ± 0.24	5/2 <sup>-</sup>	0.031±0.005
2689	1.32±0.28	2.48±0.52	-	-	0.011±0.002
2694	1.32±0.29	2.49±0.54	-	-	0.011±0.002
2706	2.46±0.29	11.55±1.23	1.69 ± 0.26	7/2 <sup>-</sup>	0.050±0.005
2721	1.41±0.24	2.72±0.47	-	-	0.012±0.002
2744	2.65±0.28	5.20±0.55	-	-	0.022±0.002
2760	1.87±0.30	3.70±0.59	-	-	0.015±0.002
2778	1.51±0.25	6.54±1.02	1.32 ± 0.29	7/2 <sup>+</sup>	0.026±0.004
2787	1.51±0.29	3.04±0.58	-	-	0.012±0.002
2798	3.32±0.31	6.77±0.62	-	-	0.027±0.002
2827	3.84±0.33	13.92±1.38	0.80 ± 0.12	5/2 <sup>+</sup>	0.053±0.005
2841	3.75±0.33	7.87±0.70	-	-	0.030±0.003
2846	1.30±0.33	2.74±0.69	-	-	0.010±0.003
2858	3.77±0.33	8.01±0.71	-	-	0.030±0.003
2863	1.48±0.23	3.15±0.50	-	-	0.012±0.002
2883	1.68±0.24	3.63±0.52	-	-	0.013±0.002
2906	1.83±0.24	4.02±0.52	-	-	0.014±0.002
2916	2.23±0.25	9.77±1.19	1.12 ± 0.19	7/2 <sup>-</sup>	0.034±0.004
2925	3.47±0.31	10.43±1.18	0.37 ± 0.07	5/2 <sup>-</sup>	0.036±0.004
3020	4.10±0.36	15.52±1.49	0.63 ± 0.09	5/2 <sup>-</sup>	0.049±0.005
3035	2.10±0.26	5.04±0.63	-	-	0.016±0.002

TABLE IV. (*Continued*).

$E_x$ (keV)	$I_s$ (eV b)	$g_J \Gamma_0$ (meV)	$R_{\text{expt}}$	Final state $J_f^\pi$	$B(M1)^\uparrow^a$ ( $\mu_N^2$ )
3040	2.48±0.27	5.95±0.65	-	-	0.018±0.002
3049	1.27±0.26	8.77±1.82	2.07 ± 0.60	7/2 <sup>+</sup>	0.027±0.006
3057	1.45±0.26	3.52±0.64	-	-	0.011±0.002
3078	1.69±0.24	7.44±1.18	0.90 ± 0.21	7/2 <sup>-</sup>	0.022±0.003
3084	2.87±0.30	15.94±1.54	1.31 ± 0.18	5/2 <sup>-</sup>	0.047±0.005
3088	2.06±0.26	5.10±0.65	-	-	0.015±0.002
3100	1.87±0.24	4.69±0.60	-	-	0.014±0.002
3106	2.64±0.38	6.63±0.95	-	-	0.019±0.003
3131	3.16±0.30	8.06±0.77	-	-	0.023±0.002
3154	1.56±0.24	4.03±0.61	-	-	0.011±0.002
3158	1.68±0.29	12.51±1.53	1.99 ± 0.39	5/2 <sup>+</sup>	0.034±0.004
3162	1.10±0.28	2.87±0.72	-	-	0.008±0.002
3228	0.88±0.20	2.39±0.54	-	-	0.006±0.001
3233	1.04±0.24	2.82±0.66	-	-	0.007±0.002
3239	1.88±0.22	5.14±0.61	-	-	0.013±0.002
3251	0.73±0.18	2.01±0.50	-	-	0.005±0.001
3268	0.71±0.21	1.99±0.59	-	-	0.005±0.001
3272	0.71±0.20	1.99±0.57	-	-	0.005±0.001
3288	1.17±0.19	3.29±0.53	-	-	0.008±0.001
3333	1.17±0.23	3.39±0.65	-	-	0.008±0.002
3346	1.47±0.22	4.28±0.65	-	-	0.010±0.001
3356	1.32±0.27	3.86±0.80	-	-	0.009±0.002
3375	0.90±0.21	2.67±0.62	-	-	0.006±0.001
3413	1.64±0.28	4.96±0.85	-	-	0.011±0.002
3456	1.24±0.26	3.84±0.81	-	-	0.008±0.002
3472	1.04±0.23	3.25±0.72	-	-	0.007±0.001
3479	0.72±0.24	2.27±0.76	-	-	0.005±0.002
3506	1.74±0.26	5.57±0.82	-	-	0.011±0.002
3528	1.01±0.23	3.26±0.74	-	-	0.006±0.001
3663	1.79±0.35	6.26±1.22	-	-	0.011±0.002
3680	2.04±0.40	7.20±1.40	-	-	0.012±0.002
3684	1.58±0.32	5.58±1.13	-	-	0.010±0.002
3713	1.84±0.33	6.62±1.17	-	-	0.011±0.002
3717	2.33±0.35	8.36±1.24	-	-	0.014±0.002
3734	1.58±0.45	5.74±1.64	-	-	0.010±0.003
3739	1.27±0.31	4.64±1.13	-	-	0.008±0.002
3775	1.17±0.39	4.35±1.43	-	-	0.007±0.002
3821	1.29±0.34	10.01±2.80	1.09 ± 0.43	5/2 <sup>-</sup>	0.016±0.004
3842	1.41±0.55	5.42±2.21	-	-	0.008±0.003

<sup>a</sup>Assuming  $M1$  transitions.

This totally different behavior of  $^{157}\text{Gd}$  as compared to the odd Dy isotopes, where a concentration of strength is observed in the region of the scissors mode, cannot simply be explained by the different possibilities for the decays of the excited states to various states in the low-lying collective bands. This is illustrated in Fig. 7 where the lowest bands in  $^{157}\text{Gd}$ ,  $^{161}\text{Dy}$ , and  $^{163}\text{Dy}$  are shown. States which were populated in the present photon scattering experiments are marked by asterisks. As can be seen, for  $^{161}\text{Dy}$  there are three low-lying bands where states can be populated by the decay from the photoexcited levels. In  $^{157}\text{Gd}$ , however, there are only two bands near the ground state. Nevertheless, the sensitivity of the  $^{161}\text{Dy}$  experiments was sufficient to detect a pronounced concentration of dipole strength. Up to now, the

reason for this different behavior of the Dy and Gd isotopes is not clear (first preliminary NRF results on  $^{155}\text{Gd}$  [61] confirm the  $^{157}\text{Gd}$  findings of an extreme fragmentation). Theoretical calculations and more systematic experimental data on odd mass nuclei are needed to provide a deeper insight into the structure of these excitations.

### C. $E1$ strength distributions in $^{162}\text{Dy}$ and $^{164}\text{Dy}$

The systematics of  $K=0$ ,  $J^\pi=1^-$  states in rare earth nuclei observed in our previous systematic photon scattering experiments [37] show that the  $K^\pi=0^-$  strength is mainly concentrated in one or two transitions near 1.5 MeV with summed strengths of  $\Sigma B(E1)^\uparrow \approx 20 \times 10^{-3} e^2 \text{ fm}^2$  (cor-

TABLE V. Results for the reaction  $^{163}\text{Dy}(\gamma, \gamma')$ . Results for the excitation energies  $E_x$ , the integrated cross sections  $I_s$ , and the reduced transition probabilities  $B(M1)\uparrow$  are given. All states decay to the ground state ( $J^\pi=5/2^-$ ). If a decay branching to another low-lying state (besides the ground state) was observed, the branching ratio  $R_{\text{expt}}$  and the spin and parity  $J_f^\pi$  of this final state is given in columns 4 and 5, respectively.

$E_x$ (keV)	$I_s$ (eV b)	$g_J\Gamma_0$ (meV)	$R_{\text{expt}}$	Final state $J_f^\pi$	$B(M1)\uparrow^a$ ( $\mu_N^2$ )
1942	11.3±1.7	11.1± 1.7	-	-	0.131 ± 0.021
2104	2.2±0.6	2.5± 0.6	-	-	0.023 ± 0.006
2180	16.4±2.1	25.9± 4.1	0.26 ± 0.06	7/2 <sup>-</sup>	0.216 ± 0.041
2213	13.9±2.2	23.6± 4.6	0.29 ± 0.07	7/2 <sup>-</sup>	0.188 ± 0.043
2472	6.3±1.0	10.0± 1.6	-	-	0.057 ± 0.009
2542	8.0±1.2	13.5± 2.0	-	-	0.071 ± 0.010
2566	5.9±1.0	10.2± 1.7	-	-	0.052 ± 0.008
2587	13.7±1.8	23.8± 3.2	-	-	0.119 ± 0.016
2918	4.6±0.8	10.1± 1.8	-	-	0.035 ± 0.006
2958	23.4±2.9	66.4± 8.6	0.36 ± 0.09	7/2 <sup>-</sup>	0.222 ± 0.033
2967	5.1±0.9	11.6± 2.0	-	-	0.038 ± 0.006
2976	4.5±0.7	10.5± 1.8	-	-	0.034 ± 0.006
3037	10.3±1.5	42.3±10.6	0.25 ± 0.04	7/2 <sup>-</sup>	0.130 ± 0.036
3045	11.7±1.6	28.3± 3.9	-	-	0.087 ± 0.012
3057	6.2±0.9	15.0± 2.3	-	-	0.045 ± 0.007
3087	4.5±0.8	39.0±10.4	2.67 ± 0.59	7/2 <sup>-</sup>	0.115 ± 0.036
3099	8.8±1.2	41.2±10.9	0.91 ± 0.18	7/2 <sup>-</sup>	0.120 ± 0.033
3107	4.7±0.8	31.0±11.4	1.40 ± 0.34	7/2 <sup>-</sup>	0.089 ± 0.030

<sup>a</sup>Assuming  $M1$  transitions.

responding to a rather high value of  $\approx 4 \times 10^{-3}$  W.u.), whereas the strength at higher energies is rather fragmented. These low-lying  $1^-$  states are discussed in terms of  $K=0$  rotational bands based on an octupole vibration as suggested by Donner and Greiner [33]. This explanation is supported by the observed linear correlation of the energies of the

$K=0, J=1_1^-$  states with the energies of closely lying  $J=3^-$  states [37]. The strengths of these  $K=0$   $E1$  excitations could be explained by an admixture of the giant dipole resonance (GDR) to these low-lying  $1^-$  states [38].

As in our previous polarization measurements in photon scattering off  $^{150}\text{Nd}$  and  $^{160}\text{Gd}$  [26,30] also in the present

TABLE VI. Results for the reaction  $^{161}\text{Dy}(\gamma, \gamma')$ . Results for the excitation energies  $E_x$ , the integrated cross sections  $I_s$ , and the reduced transition probabilities  $B(M1)\uparrow$  are given. All states decay to the ground state ( $J^\pi=5/2^+$ ). If a decay branching to another low-lying state (besides the ground state) was observed, the branching ratio  $R_{\text{expt}}$  and the spin and parity  $J_f^\pi$  of this final state is given in columns 4 and 5, respectively.

$E_x$ (keV)	$I_s$ (eV b)	$g_J\Gamma_0$ (meV)	$R_{\text{expt}}$	Final state $J_f^\pi$	$B(M1)\uparrow^a$ ( $\mu_N^2$ )
2237	3.14±0.39	4.09±0.51	-	-	0.032 ± 0.004
2250	6.69±1.38	13.34±2.38	0.53±0.13	5/2 <sup>-</sup>	0.101 ± 0.018
2346	3.92±0.53	5.62±0.76	-	-	0.038 ± 0.005
2740	1.67±0.25	3.26±0.48	-	-	0.014 ± 0.002
2748	2.95±0.44	5.79±0.86	-	-	0.024 ± 0.004
2753	6.26±0.85	12.34±1.68	-	-	0.051 ± 0.007
2775	7.19±0.85	19.06±2.88	0.35±0.10	3/2 <sup>-</sup>	0.077 ± 0.012
2812	2.84±0.62	13.16±2.11	1.35±0.33	3/2 <sup>-</sup>	0.051 ± 0.008
2820	11.88±1.24	34.11±3.80	0.41±0.07	7/2 <sup>+</sup>	0.131 ± 0.015
2838	4.09±0.68	24.73±3.63	2.04±0.44	3/2 <sup>-</sup>	0.094 ± 0.014
2849	3.14±0.67	6.64±1.41	-	-	0.025 ± 0.005
2864	11.48±1.22	31.57±4.24	0.31±0.08	3/2 <sup>-</sup>	0.116 ± 0.016
2905	2.88±0.61	13.99±1.81	0.63±0.17	3/2 <sup>-</sup>	0.049 ± 0.009
			0.82±0.23	9/2 <sup>+</sup>	
2994	2.18±0.58	5.09±0.72	-	-	0.016 ± 0.003
3113	1.59±0.24	9.64±1.56	1.36±0.32	5/2 <sup>-</sup>	0.027 ± 0.005
3155	1.91±0.28	4.94±0.51	-	-	0.013 ± 0.001
3644	2.87±0.33	9.92±1.16	-	-	0.018 ± 0.002

<sup>a</sup>Assuming  $M1$  transitions.

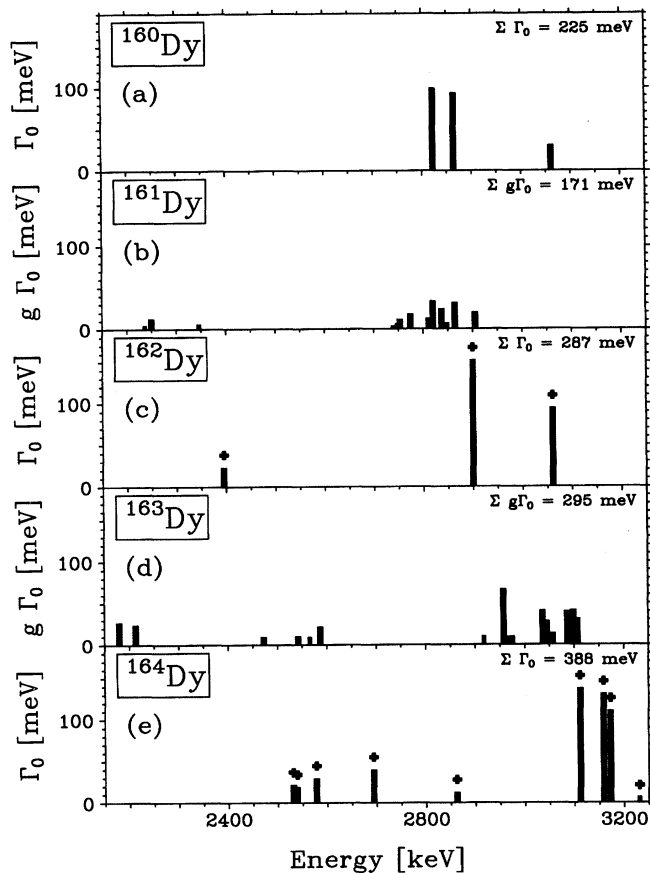


FIG. 5. Dipole strength distributions in the isotopes  $^{160,161,162,163,164}\text{Dy}$ . For the even-even isotopes the ground state widths  $\Gamma_0$  of  $\Delta K=1$  transitions are plotted. For transitions in  $^{162,164}\text{Dy}$  marked by crosses the positive parities could be determined in the present NRF polarization measurements. In the case of the odd nuclei  $^{161,163}\text{Dy}$ , because of the unknown spins of the excited states, the products of the ground state decay widths  $\Gamma_0$  and the spin factor  $g = (2J+1)/(2J_0+1)$  are plotted.

experiments on  $^{162,164}\text{Dy}$  enhanced, isolated  $E1$  excitations could be detected at excitation energies of 2.520 MeV and 2.670 MeV, respectively [see Fig. 3(c), Tables III and II]. A common feature of these strong  $E1$  excitations around 2.5 MeV in these deformed nuclei is the observation of an uncommon decay branching ratio  $R_{\text{expt}}$ . The measured branching ratios lie in between the values of 0.5 and 2 as expected from the Alaga rules for pure  $K = 1$  and  $K = 0$  states. Since

TABLE VII. Comparison of the experimental results for  $M1$  excitations in  $^{163}\text{Dy}$  with recent IBFM calculations [24]. The non-symmetric scissors mode states are denoted by ns.

$J_i \rightarrow J_f$	Decay branching $R_{\text{IBFM}}$	$B(M1) \uparrow$		States
		$B(M1) \uparrow_{\text{ns}}^{\text{theo}}$ ( $\mu_N^2$ )	$B(M1) \uparrow_{>2.6 \text{ MeV}}^{\text{expt}}$ ( $\mu_N^2$ )	
$5/2_1 \rightarrow 3/2_{\text{ns}}$	0.00	0.41	$0.24 \pm 0.04$	5
$5/2_1 \rightarrow 5/2_{\text{ns}}$	2.20	0.20	$0.20 \pm 0.07$	2
$5/2_1 \rightarrow 7/2_{\text{ns}}$	0.36	0.62	$0.47 \pm 0.10$	3
$5/2_1 \rightarrow (J_f)_{\text{ns}}$		1.23	$0.91 \pm 0.21$	10

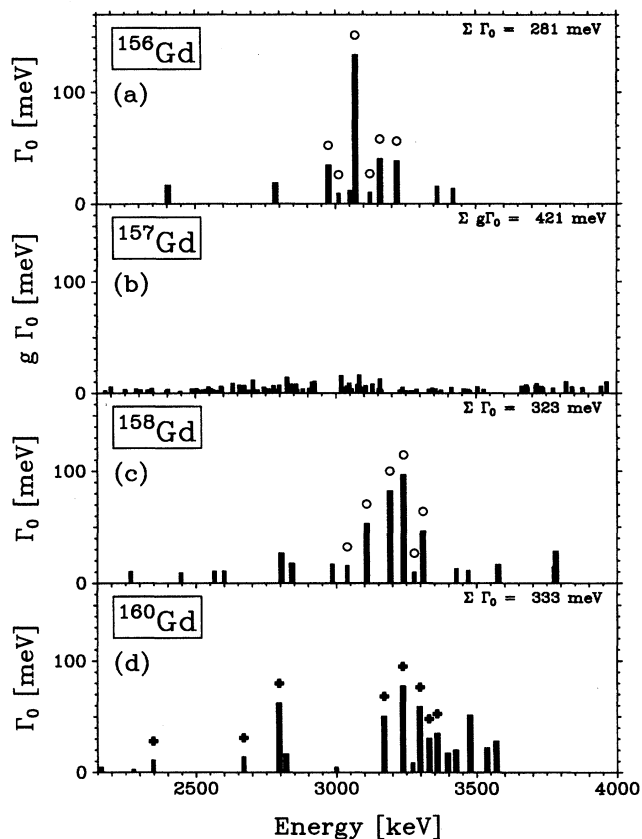


FIG. 6. Dipole strength distributions in the isotopes  $^{156,157,158,160}\text{Gd}$ . For the even-even isotopes the ground state widths  $\Gamma_0$  of  $\Delta K=1$  transitions are plotted. For transitions in  $^{160}\text{Gd}$  marked by crosses the positive parities could be determined in previous NRF polarization measurements [30]; for transitions in  $^{156,158}\text{Gd}$  marked by open symbols the positive parities are known from electron scattering experiments [28,31]. In the case of the odd nucleus  $^{157}\text{Gd}$ , because of the unknown spins of the excited states, the products of the ground state decay widths  $\Gamma_0$  and the spin factor  $g = (2J+1)/(2J_0+1)$  are plotted.

in general the branching ratios observed in these strongly deformed nuclei are in an excellent agreement with the Alaga rules, these deviations may be interpreted as a possible  $K$  mixing [62].

In Table VIII the experimental results for these  $E1$  excitations are summarized [excitation energies  $E_x$ , ground state transition widths  $\Gamma_0$ , decay branching ratios  $R_{\text{expt}}$ , and reduced transition probabilities  $B(E1) \uparrow$ ]. The transition energies and the rather high  $B(E1) \uparrow$  strength of  $3$  to  $5 \times 10^{-3} e^2 \text{ fm}^2$  may suggest an interpretation in terms of enhanced electric dipole excitations in deformed nuclei due to reflection asymmetric shapes like octupole deformations or cluster configurations [32–35,40]. Both pictures are able to explain the right order of magnitude of the observed  $E1$  strength (see, e.g., [30]). Another interpretation of these strong  $E1$  transitions is the explanation as two-phonon excitations caused by the coupling of octupole vibrations ( $K = 1$ ) to the  $K^\pi = 2^+$ ,  $\gamma$  vibration [41]. Such two-phonon excitations were theoretically explicitly treated by Donner and Greiner already in 1966. The resulting  $1^-$  states can be ex-

$^{157}\text{Gd}$	$^{161}\text{Dy}$	$^{163}\text{Dy}$
<u>5/2- 426.0</u>		<u>3/2- 389.7</u>
		<u>1/2- 351.1</u>
		<u>9/2+ 336.5</u>
<u>11/2+ 276.0</u>		<u>11/2- 281.6</u>
		<u>7/2+ 285.6</u>
<u>9/2- 227.3</u>		<u>5/2+ 250.9</u>
	<u>9/2- 201.1</u>	
<u>9/2+ 180.2</u>	<u>11/2+ 184.2</u>	<u>9/2- 167.4</u>
<u>7/2- 131.4</u>		<u>5/2- 131.7</u>
*		
<u>7/2+ 115.7</u>		
*	<u>9/2+ 100.4</u>	<u>7/2- 103.0</u>
	*	
<u>5/2- 54.5</u>		<u>3/2- 74.6</u>
*		*
<u>5/2+ 63.9</u>		<u>7/2- 73.5</u>
*		*
<u>3/2- 0</u>	<u>7/2+ 43.8</u>	<u>5/2- 0</u>
*	*	*
	<u>5/2- 25.7</u>	
	*	
	<u>5/2+ 0</u>	
	*	

FIG. 7. Comparison of low-lying collective bands in the odd neutron nuclei  $^{157}\text{Gd}$ ,  $^{161}\text{Dy}$ , and  $^{163}\text{Dy}$ . Spins, parities and excitation energies are given. States, which are fed by transitions from levels excited in the present photon scattering experiments, are marked by asterisks.

cited by dipole transitions from the ground state as a result of the coupling of the giant electric dipole resonance to the octupole vibration [33].

Unfortunately, there is not much information on the energetic positions of the  $K = 1$  octupole band heads in rare earth nuclei. Therefore, in a recent analysis [41] as possible candidates for the two-phonon  $E1$  excitations (besides known  $K = 1$  band heads) the lowest  $J^\pi = 1^-$  states above the  $K = 0$  bands were taken exhibiting an uncommon decay branching ratio. In the case of  $^{162}\text{Dy}$  all needed data on octupole bands are known from recent systematics studies using different particle induced reactions [63]. An excellent agreement of the experimentally observed excitation energies  $E_{\text{expt}}^{K=1}(1^-)$  of the assumed two-phonon excitations and the sum of the  $K = 1$  octupole and the  $\gamma$  vibrational excitations

TABLE VIII. Results for enhanced electric dipole excitation in deformed nuclei (this work and [41]): excitation energies  $E_x$ , ground state transition widths  $\Gamma_0$ , experimental decay branchings  $R_{\text{expt}} = B(1^- \rightarrow 0^+) / B(1^- \rightarrow 2^+)$ , and reduced transition probabilities  $B(E1)\uparrow$ .

Nucleus	$E_x$ (MeV)	$\Gamma_0$ (meV)	$R_{\text{expt}}$	$B(E1)\uparrow$ ( $10^{-3} e^2 \text{ fm}^2$ )
$^{150}\text{Nd}$	2.414	$14.9 \pm 2.0$	$0.86 \pm 0.09$	$3.0 \pm 0.4$
$^{160}\text{Gd}$	2.471	$16.4 \pm 2.6$	$1.56 \pm 0.21$	$3.1 \pm 0.5$
$^{162}\text{Dy}$	2.520	$30.2 \pm 4.0$	$1.31 \pm 0.08$	$5.0 \pm 0.4$
$^{164}\text{Dy}$	2.670	$27.0 \pm 4.7$	$1.32 \pm 0.14$	$4.3 \pm 0.4$

has been shown in [41]. This supports the tentative interpretation of these strong  $E1$  excitations as two-phonon excitations. Clearly, this explanation has to be corroborated by further experiments, in particular by admittedly difficult measurements of the decay branching ratios of the excited  $J^\pi = 1^-$  states to the vibrational and octupole bands.

Besides these more or less macroscopic collective descriptions, microscopic calculations for  $E1$  excitations in deformed nuclei were reported by Soloviev and co-workers [64,65]. These authors calculated within the framework of the quasiparticle-phonon-nuclear-model (QPNM) excitation energies, wave functions, and  $E1$  transition strengths for the deformed rare earth nuclei  $^{158}\text{Gd}$ ,  $^{162,164}\text{Dy}$ , and  $^{168}\text{Er}$ , explicitly. In Fig. 8 the calculations by Soloviev *et al.* [65] for  $^{164}\text{Dy}$  are compared with the results of the present NRF experiments. The  $K$  numbers were assigned according the measured branching ratios ( $R_{\text{expt}} \leq 1 \rightarrow K=1$ ;  $R_{\text{expt}} \geq 1 \rightarrow K=0$ ). In the investigated energy range below 4 MeV the calculated total  $E1$  strengths for  $K=0$  states are about a factor of 3–4 larger than for  $K=1$  states. The absolute calculated values, however, are about 3–5 times larger than the experimental ones. Therefore, keeping this scaling factor in mind, it seems to be reasonable that in the experiments on  $^{164}\text{Dy}$  no  $\Delta K=1$   $E1$  transitions could be detected.

## VI. CONCLUSION

Systematic photon scattering experiments were performed on the nuclei  $^{161,163}\text{Dy}$  and  $^{157}\text{Gd}$  to study the existence and

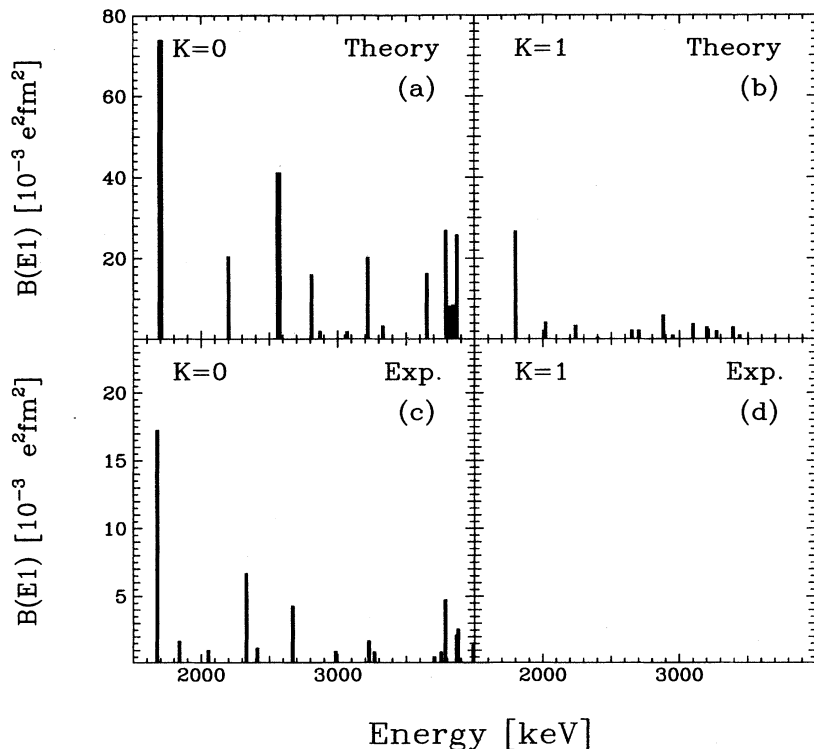


FIG. 8. Comparison of calculated  $E1$  strengths distribution for  $K=0$  and  $K=1$  transitions in  $^{164}\text{Dy}$  (upper part, from Soloviev and Sushkov [65]) with the experimental data of the present work (lower part). The scale of the abscissa in the lower part is enlarged by a factor of 3.

fragmentation of the scissors mode in odd, deformed nuclei. The experiments provided detailed information on the excitation energies and transition probabilities of low-lying dipole excitations. In the case of the even-even nuclei  $^{162,164}\text{Dy}$  in addition spins and parities of the excited states could be determined model independently. The results are compared with the systematics obtained for the neighboring even-even isotopes  $^{160}\text{Dy}$  and  $^{156,158,160}\text{Gd}$ , which were extensively studied in previous photon and electron scattering experiments. The present results show for the odd Dy isotopes a concentration of dipole strength, which fits nicely into the systematics of the orbital  $M1$  mode. However, the by a factor of 3 smaller total  $M1$  strength in the region of the scissors mode in the odd Dy isotopes as compared to their even-even neighbors has to be explained. On the other hand, the dipole strength in  $^{157}\text{Gd}$  is completely fragmented into about 90 excitations in the energy range where the scissors mode is

expected. Up to now, the reason for this completely different behavior of the odd Dy isotopes in comparison to  $^{157}\text{Gd}$  is not clear. There is a need of more experimental data and theoretical calculations to get a deeper insight into the structure of these excitations in odd nuclei and to find possible explanations for the obviously different fragmentation of the low-lying dipole strength in various odd, deformed nuclei.

#### ACKNOWLEDGMENTS

We wish to thank P. Van Isacker, R. V. Jolos, A. Richter, V. G. Soloviev, and S. W. Yates for stimulating and enlightening discussions. The help of our former co-workers W. Geiger, R. D. Heil, S. Lindenstruth, B. Schlitt, and C. Wesselborg in an early stage of the experiments is gratefully acknowledged. This work was supported in part by the Deutsche Forschungsgemeinschaft under Contract Nos. Br 799/6 and Kn 154/21.

- [1] U.E.P. Berg and U. Kneissl, *Annu. Rev. Nucl. Part. Sci.* **37**, 33 (1987).  
 [2] D. Bohle, A. Richter, W. Steffen, A.E.L. Dieperink, N. LoIudice, F. Palumbo, and O. Scholten, *Phys. Lett.* **137B**, 27 (1984).  
 [3] A. Richter, *Nucl. Phys.* **A507**, 99c (1990).  
 [4] A. Richter, *Nucl. Phys.* **A522**, 139c (1991).  
 [5] A. Richter, in *Proceedings of the International Conference on Perspectives of the Interacting Boson Model on the Occasion of its 20th Anniversary*, Padova, 1994.  
 [6] P. von Brentano, A. Zilges, R.D. Heil, R.-D. Herzberg, U. Kneissl, H.H. Pitz, and C. Wesselborg, *Nucl. Phys.* **A557**, 593c (1993).

- [7] A. Richter, *Prog. Part. Nucl. Phys.* **34**, 261 (1995).  
 [8] U. Kneissl, *Prog. Part. Nucl. Phys.* **24**, 41 (1990).  
 [9] U. Kneissl, *Prog. Part. Nucl. Phys.* **28**, 331 (1992).  
 [10] U. Kneissl, J. Margraf, H.H. Pitz, P. von Brentano, R.-D. Herzberg, and A. Zilges, *Prog. Part. Nucl. Phys.* **34**, 285 (1995).  
 [11] N. Lo Iudice and F. Palumbo, *Phys. Rev. Lett.* **41**, 1532 (1978).  
 [12] R. Nojarov, *Prog. Part. Nucl. Phys.* **34**, 297 (1995).  
 [13] F.G. Scholz, R. Nojarov, and A. Faessler, *Phys. Rev. Lett.* **63**, 1356 (1989).  
 [14] W. Ziegler, C. Rangacharyulu, A. Richter, and C. Spieler, *Phys. Rev. Lett.* **65**, 2515 (1990).  
 [15] W. Ziegler, N. Huxel, P. von Neumann-Cosel, C. Ranga-

- charyulu, A. Richter, H.J. Wörtche, and C. Spieler, Nucl. Phys. **A564**, 366 (1993).
- [16] C. Rangacharyulu, A. Richter, H.J. Wörtche, W. Ziegler, and R.F. Casten, Phys. Rev. C **43**, R949 (1991).
- [17] J. Margraf, C. Wesselborg, R.D. Heil, U. Kneissl, H.H. Pitz, C. Rangacharyulu, A. Richter, H.J. Wörtche, and W. Ziegler, Phys. Rev. C **45**, R521 (1992).
- [18] H.H. Pitz, R.D. Heil, U. Kneissl, S. Lindenstruth, U. Seemann, R. Stock, C. Wesselborg, A. Zilges, P. von Brentano, S.D. Hoblit, and A.M. Nathan, Nucl. Phys. **A509**, 587 (1990).
- [19] J. Margraf, R.D. Heil, U. Maier, U. Kneissl, H.H. Pitz, H. Friedrichs, S. Lindenstruth, B. Schlitt, C. Wesselborg, P. von Brentano, R.-D. Herzberg, and A. Zilges, Phys. Rev. C **47**, 1474 (1993).
- [20] N. Lo Iudice and A. Richter, Phys. Lett. B **304**, 193 (1993).
- [21] R.-D. Herzberg, A. Zilges, P. von Brentano, R.D. Heil, U. Kneissl, J. Margraf, H.H. Pitz, H. Friedrichs, S. Lindenstruth, and C. Wesselborg, Nucl. Phys. **A563**, 445 (1993).
- [22] N. Pietralla, P. von Brentano, R.-D. Herzberg, A. Zilges, U. Kneissl, J. Margraf, H. Maser, and H. H. Pitz, this issue, Phys. Rev. C **52**, 2317 (1995).
- [23] N. Huxel, W. Ahner, H. Diesener, P. von Neumann-Cosel, C. Rangacharyulu, A. Richter, C. Spieler, W. Ziegler, C. De Coster, and K. Heyde, Nucl. Phys. **A539**, 478 (1992).
- [24] I. Bauske, J.M. Arias, P. von Brentano, A. Frank, H. Friedrichs, R.D. Heil, R.-D. Herzberg, F. Hoyler, P. Van Isacker, U. Kneissl, J. Margraf, H.H. Pitz, C. Wesselborg, and A. Zilges, Phys. Rev. Lett. **71**, 975 (1993).
- [25] C. Wesselborg, P. von Brentano, K.O. Zell, R.D. Heil, H.H. Pitz, U.E.P. Berg, U. Kneissl, S. Lindenstruth, U. Seemann, and R. Stock, Phys. Lett. B **207**, 22 (1988).
- [26] H. Friedrichs, B. Schlitt, J. Margraf, S. Lindenstruth, C. Wesselborg, R.D. Heil, H.H. Pitz, U. Kneissl, P. von Brentano, R.D. Herzberg, A. Zilges, D. Häger, G. Müller, and M. Schumacher, Phys. Rev. C **45**, R892 (1992).
- [27] D. Bohle, G. Kuchler, A. Richter, and W. Steffen, Phys. Lett. **148B**, 260 (1984).
- [28] D. Bohle, A. Richter, U.E.P. Berg, J. Drexler, R.D. Heil, U. Kneissl, H. Metzger, R. Stock, B. Fischer, H. Hollick, and D. Kollwe, Nucl. Phys. **A458**, 205 (1986).
- [29] H.H. Pitz, U.E.P. Berg, R.D. Heil, U. Kneissl, R. Stock, C. Wesselborg, and P. von Brentano, Nucl. Phys. **A492**, 411 (1989).
- [30] H. Friedrichs, D. Häger, P. von Brentano, R.D. Heil, R.-D. Herzberg, U. Kneissl, J. Margraf, G. Müller, H.H. Pitz, B. Schlitt, M. Schumacher, C. Wesselborg, and A. Zilges, Nucl. Phys. **A567**, 266 (1994).
- [31] U. Hartmann, D. Bohle, F. Humbert, and A. Richter, Nucl. Phys. **A499**, 93 (1989).
- [32] F. Iachello, Phys. Lett. **160B**, 1 (1985).
- [33] W. Donner and W. Greiner, Z. Phys. **197**, 440 (1966).
- [34] P.D. Cottle and D. A. Bromley, Phys. Lett. B **182**, 129 (1986).
- [35] P.D. Cottle, Phys. Rev. C **42**, 1264 (1990).
- [36] P.A. Butler and W. Nazarewicz, Nucl. Phys. **A533**, 249 (1991).
- [37] A. Zilges, P. von Brentano, H. Friedrichs, R.D. Heil, U. Kneissl, S. Lindenstruth, H.H. Pitz, and C. Wesselborg, Z. Phys. A **340**, 155 (1991).
- [38] A. Zilges, P. von Brentano, and A. Richter, Z. Phys. A **341**, 489 (1992).
- [39] T. Guhr, K.-D. Hummel, G. Kilgus, D. Bohle, A. Richter, C.W. de Jager, H. de Vries, and P.K.A. de Witt Huberts, Nucl. Phys. **A501**, 95 (1989).
- [40] I. Ahmad and P.A. Butler, Annu. Rev. Nucl. Part. Sci. **43**, 71 (1993).
- [41] U. Kneissl, A. Zilges, J. Margraf, I. Bauske, P. von Brentano, H. Friedrichs, R.D. Heil, R.-D. Herzberg, H.H. Pitz, B. Schlitt, and C. Wesselborg, Phys. Rev. Lett. **71**, 2180 (1993).
- [42] L.W. Fagg and S.S. Hanna, Rev. Mod. Phys. **31**, 711 (1959).
- [43] K. Siegbahn,  $\alpha, \beta, \gamma$  - Spectroscopy (North-Holland, Amsterdam, 1965), p. 1197.
- [44] A.H. Wapstra, G.J. Nijgh, and R. van Lieshout, Nuclear Spectroscopy Tables (North-Holland, Amsterdam, 1959).
- [45] U. Kneissl, Nucl. Phys. News **4**, 24 (1994).
- [46] G. Alaga, K. Alder, A. Bohr, and B.R. Mottelson, Dan. Mat. Fys. Medd. **29**, 1 (1955).
- [47] B. Schlitt, U. Maier, H. Friedrichs, S. Albers, I. Bauske, P. von Brentano, R.D. Heil, R.-D. Herzberg, U. Kneissl, J. Margraf, H.H. Pitz, C. Wesselborg, and A. Zilges, Nucl. Instrum. Methods Phys. Res. A **337**, 416 (1994).
- [48] H. Maser, Diploma thesis, Stuttgart, 1993, unpublished.
- [49] P.M. Endt and C. van der Leun, Nucl. Phys. **A310**, 1 (1978).
- [50] S. Lindenstruth, A. Degener, R.D. Heil, A. Jung, U. Kneissl, J. Margraf, H.H. Pitz, H. Schacht, U. Seemann, R. Stock, and C. Wesselborg, Nucl. Instrum. Methods Phys. Res. A **300**, 293 (1991).
- [51] N. Pietralla, I. Bauske, O. Beck, P. von Brentano, W. Geiger, R.-D. Herzberg, U. Kneissl, J. Margraf, H. Maser, H.H. Pitz, and A. Zilges, Phys. Rev. C **51**, 1021 (1995).
- [52] M. Rittner, Diploma thesis, Stuttgart, 1994, unpublished.
- [53] D. Bohle, G. Kilgus, A. Richter, C.W. de Jager, and H. de Vries, Phys. Lett. B **195**, 326 (1987).
- [54] S.W. Yates, D.P. DiPrete, E.L. Johnson, E.M. Baum, C.A. McGrath, D. Wang, M.F. Villani, T. Belgia, B. Fazekas, and G. Molnár, in Proceedings of the IVth International Conference on Selected Topics in Nuclear Structure, Dubna, Russia, 1994; S.W. Yates, private communication.
- [55] D. Frekers, D. Bohle, A. Richter, R. Abegg, R.E. Azuma, A. Celler, C. Chan, T.E. Drake, K.P. Jackson, C.A. Miller, R. Schubank, J. Watson, and S. Yen, Phys. Lett. B **218**, 439 (1989).
- [56] J.S. Freeman, R. Chapman, J.L. Durell, M.A.C. Hotchkis, F. Khazaie, J.C. Lisle, J.N. Mo, A.M. Bruce, R.A. Cunningham, P.V. Drumm, D.D. Warner, and J.D. Garrett, Phys. Lett. B **222**, 347 (1989).
- [57] T. Eckert, Diploma thesis, Stuttgart, 1994, unpublished.
- [58] P. van Isacker and A. Frank, Phys. Lett. B **225**, 1 (1989).
- [59] A. Frank, J.M. Arias, and P. van Isacker, Nucl. Phys. **A531**, 125 (1991).
- [60] A.A. Raduta and D.S. Delion, Nucl. Phys. **A513**, 11 (1990).
- [61] A. Nord, Diploma Thesis, Stuttgart, 1995, unpublished.
- [62] A. Zilges, P. von Brentano, A. Richter, R.D. Heil, U. Kneissl, H.H. Pitz, and C. Wesselborg, Phys. Rev. C **42**, 1945 (1990).
- [63] J. Berzins, P. Prokofjevs, R. Georgii, R. Hucke, T. von Egidy, G. Hlawatsch, J. Klor, H. Lindner, U. Mayerhofer, H.H. Schmidt, A. Walter, V.G. Soloviev, N.Yu. Shirikova, and A.V. Sushkov, Nucl. Phys. **A584**, 413 (1995).
- [64] V.G. Soloviev and A.V. Sushkov, Phys. Lett. B **262**, 189 (1991).
- [65] V.G. Soloviev and A.V. Sushkov, Phys. At. Nucl. **57**, 1304 (1994).